

Implications for the Cosmic Reionization from the Optical Afterglow Spectrum of the Gamma-Ray Burst 050904 at $z = 6.3^*$

Tomonori TOTANI¹, Nobuyuki KAWAI², George KOSUGI³, Kentaro AOKI⁴, Toru YAMADA³,
Masanori IYE³, Kouji OHTA¹, and Takashi HATTORI⁴

¹*Department of Astronomy, Kyoto University, Sakyo-ku, Kyoto 606-8502*
totani@kusastro.kyoto-u.ac.jp

²*Department of Physics, Tokyo Institute of Technology, 2-12-1 Ookayama, Meguro-ku, Tokyo 152-8551*

³*National Astronomical Observatory of Japan, 2-21-1 Osawa, Mitaka, Tokyo 181-8588*

⁴*Subaru Telescope, National Astronomical Observatory of Japan, Hilo, HI 96720, USA*

(Received ; accepted)

Abstract

The gamma-ray burst (GRB) 050904 at $z = 6.3$ provides the first opportunity of probing the intergalactic medium (IGM) by GRBs at the epoch of the reionization. Here we present a spectral modeling analysis of the optical afterglow spectrum taken by the Subaru Telescope, aiming to constrain the reionization history. The spectrum shows a clear damping wing at wavelengths redward of the Lyman break, and the wing shape can be fit either by a damped Ly α system with a column density of $\log(N_{\text{HI}}/\text{cm}^{-2}) \sim 21.6$ at a redshift close to the detected metal absorption lines ($z_{\text{metal}} = 6.295$), or by almost neutral IGM extending to a slightly higher redshift of $z_{\text{IGM,u}} \sim 6.36$. In the latter case, the difference from z_{metal} may be explained by acceleration of metal absorbing shells by the activities of the GRB or its progenitor. However, we exclude this possibility by using the light transmission feature around the Ly β resonance, leading to a firm upper limit of $z_{\text{IGM,u}} \leq 6.314$. We then show an evidence that the IGM was largely ionized already at $z = 6.3$, with the best-fit neutral fraction of IGM, $x_{\text{HI}} = 0.00$, and upper limits of $x_{\text{HI}} < 0.17$ and 0.60 at 68 and 95% C.L., respectively. This is the first direct and quantitative upper limit on x_{HI} at $z > 6$. Various systematic uncertainties are examined, but none of them appears large enough to change this conclusion. To get further information on the reionization, it is important to increase the sample size of $z \gtrsim 6$ GRBs, in order to find GRBs with low column densities ($\log N_{\text{HI}} \lesssim 20$) within their host galaxies, and for statistical studies of Ly α line emission from host galaxies.

Key words: cosmology: early universe — gamma rays: observations — gamma rays: theory — galaxies: intergalactic medium

1. Introduction

Although more than 30 years have passed since the discovery of gamma-ray bursts (GRBs) (Klebesadel, Strong, & Olson 1973, see, e.g., Mészáros 2002; Piran 2004 for recent reviews), it was rather recent that GRBs became widely recognized as a unique tool of cosmological studies and exploring the early universe. It was just before GRBs were proven to have the cosmological origin (Metzger et al. 1997) that the first attempt to study the cosmic star formation history by using GRBs was made (Totani 1997; Wijers et al. 1998). The potential use of GRBs as a probe of the reionization history of the intergalactic medium (IGM) was also pointed out (Miralda-Escudé 1998), but at that time, it was thought that GRBs can probe the universe at most up to modest redshifts of $z \sim 3$ by instruments available at that time or in the near future. Such notion was, however, soon discarded by the discoveries of extremely luminous GRBs like GRB 971214 (Kulkarni et al. 1998) and 990123 (Kulkarni et al. 1999), which could

be detected even at redshifts beyond 10. Then it did not take long time before astrophysicists started to discuss GRBs as a promising lighthouse to study the extremely high redshift universe, potentially giving cosmologically important information including the population III star formation and the reionization history (Lamb & Reichart 2000; Ciardi & Loeb 2000).

During 2000–2004, satellites such as the BeppoSAX and the HETE-2 continued to discover more and more GRBs, and there was important progress including the establishment of the firm connection between long duration GRBs and energetic supernovae (Stanek et al. 2003; Hjorth et al. 2003a). However, the distance of GRBs did not extend to very high redshift, with the highest record of $z = 4.5$ (Andersen et al. 2000). The launch of the Swift satellite in 2004 then allowed the GRB community to search for fainter and more distant GRBs with improved detection rate. The GRB 050904 was discovered by the Swift on 2005 September 4 at 01:51:44 UT (Cusumano et al. 2005), and follow-up photometric observations of the afterglow found a strong spectral break between optical and near-infrared (NIR) bands, indicating a very high redshift of $z \sim 6$ (Haislip et al. 2005; Price

* Based on data collected at the Subaru Telescope, which is operated by the National Astronomical Observatory of Japan.

et al. 2005; Tagliaferri et al. 2005). This suggestion was confirmed by the subsequent spectroscopic observation by the Subaru Telescope, which found metal absorption lines at $z = 6.295$ and the corresponding Lyman break and red damping wing (Kawai et al. 2005, hereafter Paper I). This opens a new era of GRB observations at redshifts that are close to the cosmic reionization and comparable to those of the most distant galaxies (Taniguchi et al. 2005) and quasars (White et al. 2003; Fan et al. 2006). Here we report a detailed analysis and interpretation of the optical afterglow spectrum of GRB 050904 presented in Paper I, to derive implications for the reionization.

The famous Gunn-Peterson (GP) test tells us that the IGM is highly ionized at $z \lesssim 5$ (Gunn & Peterson 1965), while the observations of the cosmic microwave background radiation (CMB) indicates that the universe became neutral at the recombination epoch of $z \sim 1100$ (Spergel et al. 2003). The reionization of the IGM is believed to have occurred during $z \sim 6$ –20 by the first stars and/or quasars, and the precise epoch and nature of the reionization is one of the central topics in the modern cosmology (see Loeb & Barkana 2001; Barkana & Loeb 2001; Miralda-Escudé 2003; Haiman 2004 for recent reviews). The dramatic increase of the optical depth of the Ly α forest with increasing redshift at $z \gtrsim 5.2$ (Djorgovski et al. 2001) and the subsequent discovery of broad and black troughs of Ly α absorption (the GP troughs) in the spectra of $z \gtrsim 6$ quasars (Becker et al. 2001; White et al. 2003; Fan et al. 2003, 2006) indicate that we are beginning to probe the epoch of reionization (Fan et al. 2002; Cen & McDonald 2002; but see also Songaila & Cowie 2002). On the other hand, the polarization observation of the CMB by the Wilkinson Microwave Anisotropy Probe (WMAP) indicates a much higher redshift of reionization, $z = 17 \pm 5$ (Kogut et al. 2003). Some theorists have argued that the hydrogen in the IGM could have been reionized twice (Wyithe & Loeb 2003; Cen 2003).

Because the cross section of the Ly α resonance absorption is so large, the light blueward of the Ly α wavelength at the source is completely attenuated if the IGM neutral fraction $x_{\text{HI}} \equiv n_{\text{HI}}/n_{\text{H}}$ is larger than $\sim 10^{-3}$, and hence the Ly α trough of $z \sim 6$ quasars gives a constraint of only $x_{\text{HI}} \gtrsim 10^{-3}$. The cross section becomes much smaller for longer wavelength photons than the Ly α resonance, and the spectral shape of the red damping wing of the GP trough can potentially be used to measure x_{HI} more precisely (Miralda-Escudé 1998). However, applying this method to quasars is problematic because of the uncertainties in the original unabsorbed quasar spectra and the proximity effect (Bajtlik, Duncan, & Ostriker 1988), i.e., the ionization of surrounding IGM by strong ionizing flux from quasars (Cen & Haiman 2000; Madau & Rees 2000). Therefore, though some authors suggested $x_{\text{HI}} \gtrsim 0.1$ using $z \sim 6$ quasar spectra (Mesinger & Haiman 2004; Wyithe & Loeb 2004; Wyithe, Loeb, & Carilli 2005), these estimates are generally model dependent.

The Ly α line emission is seriously attenuated if it is embedded in the neutral IGM, and hence the Ly α line emissivity of galaxies at $z \gtrsim 6$ is another probe of the reioniza-

tion. Therefore the detection of Ly α emission from many galaxies at $z \gtrsim 6$ (Hu et al. 2002; Kodaira et al. 2003; Taniguchi et al. 2005) may indicate that the universe had already been largely ionized at that time (Malhotra & Rhoads 2004; Stern et al. 2005; Haiman & Cen 2005). However it should not be naively interpreted as implying small x_{HI} , since these Ly α emitters (LAEs) are selected by strong Ly α emission and hence they may be biased to those in ionized bubbles created by themselves or clusters of undetected sources (Haiman 2002; Wyithe & Loeb 2005). On the other hand, the Lyman-break galaxies (LBGs) selected by broad-band colors are free from the selection bias about Ly α emission, but the statistical nature of Ly α emission from LBGs at $z \gtrsim 5$ is not yet well understood (Ando et al. 2004; Bouwens et al. 2004; Dickinson et al. 2004; Giavalisco et al. 2004; Stanway et al. 2004), compared with those at $z \sim 3$ (Shapley et al. 2003). Furthermore, the Ly α line emission from lower-redshift starburst galaxies is often redshifted with respect to the systemic velocity of galaxies (e.g., Pettini et al. 2000), and such a relative redshift will lead to a higher detectability of LAEs at $z \gtrsim 6$, indicating a possible systematic uncertainty in the reionization study by Ly α emission.

GRBs have a few advantages as a probe of the cosmic reionization, compared with quasars or LAEs/LBGs. GRB afterglows are much brighter than LAEs/LBGs and comparable to or even brighter than quasars if they are observed quickly enough after the explosion. The Ly α or ultraviolet luminosity of host galaxies is irrelevant to the detectability of GRBs, and hence GRBs can probe less biased regions in the early universe, while quasars and bright LAEs/LBGs are likely biased to regions of rapid structure formation with strong clustering. In most cases it is expected that the IGM ionization state around GRB host galaxies had not yet been altered by strong ionizing flux from quasars. Finally, the spectrum of GRB afterglows has a much simpler power-law shape than complicated lines and continuum of quasars and LAEs/LBGs, and hence model uncertainty can greatly be reduced. Especially, a detailed fitting analysis of the damping wing of the GP trough in an afterglow spectrum may lead to a precise determination of x_{HI} .

In this paper we take these advantages for the first time and derive the first implications for the reionization from GRBs by using the spectrum of GRB 050904. In §2, we briefly describe the overall features of the observed spectrum. Formulations of the model fitting will be given in §3. Before the fitting, theoretically possible ranges of some model parameters will be defined (§4). Following the description of the fitting procedure (§5.1), the fitting results to the red damping wing will be given in §5.2 and §5.3. The additional constraint from the Ly β feature is discussed in §5.4. We then derive a quantitative constraint on the IGM neutral fraction, taking into account all constraints and identified uncertainties in §6. In §7 we discuss the prospects of the future GRB data as the reionization probe, based on the lessons from this first data set; §7.1 is for the neutral hydrogen column density within host

galaxies, and §7.2 is for the Ly α line emission from host galaxies. A summary and conclusions will be presented in §8.

Throughout this paper, we use the WMAP values of the cosmological parameters in the flat universe: $H_0 = 71 \text{ km s}^{-1} \text{ Mpc}^{-1}$, $\Omega_B = 0.044$, and $\Omega_M = 0.27$ (Spergel et al. 2003), and the primordial helium mass fraction in the total cosmic baryon, $Y_p = 0.25$ (Kawasaki, Kohri, & Moroi 2005).

2. The Afterglow Spectrum of GRB 050904

Figure 1 presents the spectrum of GRB 050904 at wavelengths longer than the Lyman break, taken by the FOCAS instrument (Kashikawa et al. 2002) mounted on the Subaru Telescope (Iye et al. 2004). Figure 2 presents the close-ups of the Ly α and Ly β resonance regions. See Paper I for the spectrum in the full wavelength range, the details of the observation, and basic results including the list of line detections. The pixel scale is 2.67 \AA/pix and the wavelength resolution of the spectrum is 8.5 \AA (FWHM) at $\lambda_{\text{obs}} \sim 9000 \text{ \AA}$. The total exposure time is 4.0 hours and the mid time of the exposure was September 7, 12:05 UT (3.4 days after the burst).

A clear damping wing is seen only redward of $\lambda_{\text{obs}} \sim 8900 \text{ \AA}$, corresponding to the Ly α wavelength $\lambda_\alpha = c/\nu_\alpha = 1215.67 \text{ \AA}$ at the redshift of the identified metal absorption lines, $z_{\text{metal}} = 6.295$. All the metal lines were identified at the same redshift within the error of ± 0.002 , except for an intervening absorption line system at $z = 4.840$. We searched any time variability of the damping wing shape and the absorption line strength by separating the spectrum into the first 1.5 hrs, the mid 1 hr, and the final 1.5 hrs, but statistically significant variability was not found.

At wavelengths redward of the Ly α , the spectral energy distribution (SED) has almost no feature except for the damping wing and the metal absorption lines, as expected from the power-law SED of GRB afterglows. There are some apparent emission-like features at $\lambda_{\text{obs}} \sim 8820\text{--}8920 \text{ \AA}$, which may be Ly α emission. However, the data of this wavelength range is relatively noisy and we cannot confirm these signals to be real. (See the error and the CCD image of the spectrum shown in Fig. 2.) We thus set only a conservative upper limit on the possible Ly α emission (§7.2).

In wavelengths blueward of the Ly α , the spectrum remarkably resembles those of quasars at similar redshifts. The deep, black Ly α trough can be seen in $\lambda_{\text{obs}} \sim 8500\text{--}8900 \text{ \AA}$ where the flux level is consistent with zero. On the other hand, transmission of the afterglow light can be seen in $\sim 7500\text{--}8500 \text{ \AA}$ (Paper I), implying that the universe became more transparent against the Ly α absorption at $z \lesssim 6$. The transmission, however, again disappears at $\lambda_{\text{obs}} \lesssim 7500 \text{ \AA}$ corresponding to the expected trough by the Ly β absorption.

3. Spectral Modeling

The clear red damping wing tells us the existence of a large amount of neutral hydrogen along the line of sight to the GRB. There are two possibilities for the location of the neutral hydrogen. One is a damped Ly α system (DLA) associated with the host galaxy, as often seen in the optical spectra of high redshift GRB afterglows (Jensen et al. 2001; Fynbo et al. 2001; Møller et al. 2002; Hjorth et al. 2003b; Vreeswijk et al. 2004; Chen et al. 2005; Starling et al. 2005; Vreeswijk et al. 2005; Watson et al. 2005b; Berger et al. 2005a). The other is the absorption by neutral hydrogen in the IGM before the completion of the reionization, as discussed in §1. Here we try to fit these two components to the observed shape of the damping wing, and constrain the parameters of the neutral hydrogen column density of the DLA, N_{HI} (in cm^{-2}), and the neutral hydrogen fraction in the IGM, x_{HI} .

We assume the original afterglow spectrum before absorptions as $F_\nu \propto \nu^{\beta_0}$ with the intrinsic power index of β_0 . There are a few reports of β_{obs} in the NIR bands based on color observations: $\beta_{\text{obs}} = -1.25^{+0.15}_{-0.14}$ at 10.6 hrs (Haislip et al. 2005), $\beta_{\text{obs}} = -0.3 \pm 0.6$ at 0.51 days (Price et al. 2005), and $\beta_{\text{obs}} = -1.25 \pm 0.25$ at 1.155 days (Tagliaferri et al. 2005). The NIR colors do not show any indication of extinction at the host galaxy (Tagliaferri et al. 2005). The X-ray data taken by the Swift shows a large soft X-ray absorption corresponding to $\log N_{\text{HI}} = 22.86$ in the first ~ 250 s from the trigger, but it disappears from the data after ~ 500 s with an upper bound of $\log N_{\text{HI}} < 21.57$ (Boër et al. 2005), corresponding to a visual extinction of $A_V < 2.1$ by the standard correlation for the solar abundance (Predehl & Schmitt 1995)¹. Later in this paper we will find that $\log N_{\text{HI}} \lesssim 21.6$ from the fitting to the observed damping wing shape, and metallicity of $Z \sim 0.1(N_{\text{HI}}/10^{21.6})^{-1}Z_\odot$ from the SII column density. By using the relation inferred for the Small Magellanic Cloud (SMC) having a similar metallicity (Bouchet et al. 1985), the HI column density translates to $A_V \lesssim 0.3$. In fact, the observed reddening of optical GRB afterglows is generally even smaller than those expected from the corresponding X-ray absorption or column densities of HI or metals (Galama & Wijers 2001; Savaglio & Fall 2004; Watson et al. 2005b; De Pasquale et al. 2005), possibly due to sublimation of dust grains by strong GRB radiation (Waxman & Draine 2000; Fruchter et al. 2001). Therefore we assume $A_V = 0$ at the host galaxy in our baseline model.

According to the standard synchrotron shock model of GRB afterglows (Sari, Piran, & Narayan 1998), the observed index is rather soft corresponding to the electron spectral index of $p = 2\beta_0 - 1 \sim -3.5$, indicating that the frequency of the cooling break in the afterglow SED had

¹ The column densities derived by Boër et al. (2005) are also assuming the solar abundance (M. Boër, a private communication). Since the soft X-ray absorption is dominated by metals, this conversion is not sensitive to a hydrogen-to-metal conversion (e.g., Watson et al. 2005b). On the other hand, the detection of X-ray absorption for GRB 050904 may not be significant (see Watson et al. 2005a).

already passed through the NIR bands to longer wavebands. Therefore we do not expect a spectral change between the epochs of the photometric observations and our spectroscopic observation. We then take $\beta_0 = -1.25$ in our baseline model. However, both the change of β_0 and the effect of possible reddening by dust in the host galaxy will be discussed later.

The optical depth of the DLA is calculated in the standard manner: $\tau_{\text{DLA}}(\lambda_{\text{obs}}) = N_{\text{HI}} \sigma_{\alpha} [\nu_{\text{obs}}(1+z_{\text{DLA}})]$, where $\nu_{\text{obs}} = c/\lambda_{\text{obs}}$ is the observed frequency and z_{DLA} is the redshift of the DLA. The damping wing shape is much wider than the Doppler broadening by a reasonable velocity dispersion ($\sim 3 \text{ \AA}$ for 100 km/s), and hence we ignore it. We use the exact formula of the Ly α absorption cross section for a restframe frequency ν :

$$\sigma_{\alpha}(\nu) = \frac{3\lambda_{\alpha}^2 f_{\alpha} \Lambda_{\text{cl},\alpha}}{8\pi} \frac{\Lambda_{\alpha}(\nu/\nu_{\alpha})^4}{4\pi^2(\nu - \nu_{\alpha})^2 + \Lambda_{\alpha}^2(\nu/\nu_{\alpha})^6/4}, \quad (1)$$

where $f_{\alpha} = 0.4162$ and $\Lambda_{\alpha} = 3(g_u/g_l)^{-1} f_{\alpha} \Lambda_{\text{cl},\alpha}$ are the absorption oscillator strength and the damping constant of the Ly α resonance (Peebles 1993; Madau & Rees 2000), respectively, and g_u and g_l ($g_u/g_l = 3$ for Ly α) are the statistical weights for the upper and lower levels, respectively (Cox 2000). Here, the classical damping constant is $\Lambda_{\text{cl},\alpha} = (8\pi^2 e^2)/(3m_e c \lambda_{\alpha}^2) = 1.503 \times 10^9 \text{ s}^{-1}$, where e and m_e are the electron charge and mass, respectively.

For the optical depth of the red damping wing by IGM absorption, we use the formula given by Miralda-Escudé (1998):

$$\tau_{\text{IGM}}(\lambda_{\text{obs}}) = \frac{x_{\text{HI}} R_{\alpha} \tau_{\text{GP}}(z_{\text{host}})}{\pi} \left(\frac{1+z_{\text{obs}}}{1+z_{\text{host}}} \right)^{3/2} \times \left[I \left(\frac{1+z_{\text{IGM,u}}}{1+z_{\text{obs}}} \right) - I \left(\frac{1+z_{\text{IGM,l}}}{1+z_{\text{obs}}} \right) \right], \quad (2)$$

where $(1+z_{\text{obs}}) \equiv \lambda_{\text{obs}}/\lambda_{\alpha}$, $R_{\alpha} \equiv \Lambda_{\alpha} \lambda_{\alpha}/(4\pi c) = 2.02 \times 10^{-8}$ and z_{host} is the redshift of the GRB host galaxy. In this formula, the IGM is assumed to be uniformly distributed in a redshift range from $z_{\text{IGM,l}}$ to $z_{\text{IGM,u}}$. Since the damping wing is by definition optically thin, the clumpiness of the IGM does not have significant effect. We can get a reasonable constraint on the mass-weighted optical depth by assuming a uniform distribution, which is another advantage of using the damping wing. The function $I(x)$ is given by:

$$I(x) = \frac{x^{9/2}}{1-x} + \frac{9}{7}x^{7/2} + \frac{9}{5}x^{5/2} + 3x^{3/2} + 9x^{1/2} - \frac{9}{2} \ln \frac{1+x^{1/2}}{1-x^{1/2}}, \quad (3)$$

which is almost always a sufficiently good approximation under the condition of $(z_{\text{obs}} - z_{\text{IGM,u}}) \gg R_{\alpha}(1+z_{\text{obs}})$. The Gunn-Peterson optical depth is given as:

$$\tau_{\text{GP}}(z) = \frac{3f_{\alpha} \Lambda_{\text{cl},\alpha} \lambda_{\alpha}^3 \rho_c \Omega_B (1-Y_p)}{8\pi m_p H_0 \Omega_M^{1/2}} (1+z)^{3/2} \quad (4)$$

$$= 3.88 \times 10^5 \left(\frac{1+z}{7} \right)^{3/2}, \quad (5)$$

where m_p is the proton mass and $\rho_c \equiv 3H_0^2/(8\pi G)$ is the standard critical density of the universe at the present time. The 1σ uncertainty of this numerical factor coming from the estimated errors of the cosmological parameters (Spergel et al. 2003; Kawasaki, Kohri, & Moroi 2005) is less than 8%. It should be noted that, even though the dependence on z_{host} appears explicitly in eq. (2) by the normalization of τ_{GP} at the host redshift, it actually cancels out with the factor $(1+z_{\text{host}})^{-3/2}$ in eq. (2) and hence τ_{IGM} depends only on $z_{\text{IGM,l}}$ and $z_{\text{IGM,u}}$. Therefore z_{host} is not included in our fitting parameters. We set $z_{\text{IGM,l}} = 6$, and dependence on this parameter will be discussed later. The possible range of $z_{\text{IGM,u}}$ will be discussed in detail in §4.

Although the neutral fraction x_{HI} cannot exceed the unity, what is relevant for the IGM absorption is the absolute density of neutral hydrogen rather than the neutral fraction, and the total cosmic hydrogen density depends on the cosmological parameters. Therefore, we allow $x_{\text{HI}} > 1$ in this paper, as a parameter meaning the neutral hydrogen density normalized by the total hydrogen density estimated from the standard values of the cosmological parameters.

4. Possible Ranges of z_{DLA} and $z_{\text{IGM,u}}$

Now we have the primary fitting parameters of N_{HI} , z_{DLA} , x_{HI} , and $z_{\text{IGM,u}}$. Though z_{DLA} and $z_{\text{IGM,u}}$ can be treated as free parameters in the fitting, metal absorption lines at $z_{\text{metal}} = 6.295$ have been clearly detected in the spectrum of GRB 050904. Therefore theoretical expectation and possible ranges of z_{DLA} and $z_{\text{IGM,u}}$ with respect to z_{metal} should be discussed.

The most clearly detected feature is Si II $\lambda 1259.5$ + Si II $\lambda 1260.4$, and Si II $\lambda 1253.8$ and Si II* $\lambda 1264.7$ are also detected beside the 1260 \AA feature. The profile fitting and curve of growth analysis revealed that these lines are not heavily saturated and only marginally resolved, giving column densities of $\log N_{\text{SiII}} = 15.60_{-0.17}^{+0.14}$ and $\log N_{\text{SiII}} = 14.29_{-0.39}^{+0.57}$ and a velocity dispersion of \lesssim a few hundreds km/s (Paper I). The fine-structure silicon, Si II*, is often detected in GRB afterglow spectra (Vreeswijk et al. 2004; Chen et al. 2005; Berger et al. 2005a, b) and indicates a high density environment, while it has never been clearly detected from DLAs in quasar (QSO) spectra. This suggests that the metal absorption system is a high density gas at the vicinity of the GRB explosion site (such as star forming regions, molecular clouds, or shells ejected by the GRB progenitor's activity), rather than by absorption on a galactic scale of the host galaxy or by an intervening system.

4.1. z_{DLA} versus z_{metal}

A clearly reasonable assumption is $z_{\text{DLA}} = z_{\text{metal}}$, because no metal absorption lines were identified at redshifts different from 6.295, except for the intervening system with a very different redshift, $z = 4.840$. Later we will

find that $\log N_{\text{HI}} \sim 21.6$ is necessary² to explain the observed damping wing shape by the DLA absorption with $z_{\text{DLA}} = z_{\text{metal}}$. This column density is typical for DLAs found in GRB afterglows (Vreeswijk et al. 2004), and is also similar to those of molecular clouds in the Galaxy (Larson 1981; Solomon et al. 1987). This is consistent with the high density inferred from the Si II* detection. Adopting this hydrogen column density, we get the metallicity estimates as $[\text{S}/\text{H}] = -1.3$ and $[\text{Si}/\text{H}] = -2.9$, using the solar abundance of Grevesse & Sauval (1998). Here we made no correction for ionization, assuming that the column densities of the singly ionized ions are equal to the total column densities, which is a reasonable assumption for silicon and sulphur in regions of large HI absorption like DLAs (Viegas 1995; Vladilo et al. 2001). Sulphur is not depleted to dust grains and the metallicity inferred from $[\text{S}/\text{H}]$ is reasonable compared with those found in other GRB-DLAs. (See Vreeswijk et al. 2004 for a compilation of metallicities of GRB-DLAs and QSO-DLAs.) The large depletion of silicon compared with sulphur is not surprising, since large dust depletions compared with QSO-DLAs have been observed in a few GRB afterglows (Savaglio, Fall, & Fiore 2003). Therefore the observed column densities and metallicities are reasonable in the case of the physical association between the DLA and absorption lines.

On the other hand, it seems rather unlikely that the DLA and the metal lines have different redshifts, again from the metallicity argument. In this case, no detectable lines associated with the DLA set 2σ upper limits on metallicities as $[\text{S}/\text{H}] \leq -1.5$ and $[\text{Si}/\text{H}] \leq -3.1$, while the metallicity of the region associated with the metal lines would become larger than those estimated above. Hence there must be a large metallicity difference between the DLA and the metal absorption system. Such metallicity inhomogeneity seems rather unlikely if the DLA is also physically associated with the high density region in the vicinity of the GRB. On the other hand, if the DLA is a system on the galactic scale like QSO-DLAs in the host galaxy or in any intervening galaxies, we do not expect heavy depletion of Si (Savaglio et al. 2003), and hence the upper limit on $[\text{Si}/\text{H}]$ should not be far from the total metallicity. However, such a low metallicity is not observed in any QSO-DLAs at $z \sim 1-5$, though there is no measurements of QSO-DLA metallicity at $z > 6$ (Prochaska et al. 2003). Based on these considerations, we set $z_{\text{DLA}} = z_{\text{metal}}$ in our baseline model.

However, we conservatively allow the case of $z_{\text{DLA}} = z_{\text{host}} \neq z_{\text{metal}}$, supposing that the absorbing neutral hydrogen is distributed on the scale of the host galaxy. Though a naive expectation is $z_{\text{host}} = z_{\text{metal}}$, we expect a systemic velocity difference between them up to a few hundreds km/s depending on the host galaxy's circular velocity

($|z_{\text{host}} - z_{\text{metal}}| \lesssim 0.005$). Furthermore, absorption lines blueshifted up to $\sim 3,000$ km/s with respect to the rest-frame of the host galaxy were observed in the afterglow spectrum of GRB 021004, which may have been accelerated by activities of the GRB or its progenitor (Møller et al. 2002; Schaefer et al. 2003; Mirabal et al. 2003). Similar features were found also for GRB 020813 (Barth et al. 2003) and GRB 030226 (Klose et al. 2004). The blueshifted metal lines in the GRB 021004 spectrum were highly ionized (C IV and Si IV), but Ly α absorption was observed as well at the same relative velocity. This indicates that the accelerated absorber is a mixture of neutral and highly ionized gas, and it is not unreasonable if blueshifted Si II is detected in some other GRBs.

There are, however, two arguments disfavoring the blueshift of $\sim 3,000$ km/s. First, it seems rather unlikely that only metals in such a high velocity shell were detected without any detection at other velocities or the burst restframe. Second, such high velocity shells are expected only within ~ 1 pc from the burster (Schaefer et al. 2003; Mirabal et al. 2003), which might be inconsistent with the large amount of the silicon depletion, because strong GRB radiation would destruct dust grains within ~ 1 pc of a burster (Waxman & Draine 2000; Fruchter et al. 2001; Draine & Hao 2002). However, a detailed modeling is required to examine these possibilities more quantitatively, and here we allow a blueshift of z_{metal} up to $(z_{\text{host}} - z_{\text{metal}}) \sim +0.07$. Therefore, the possible range of z_{DLA} becomes $-0.005 \lesssim (z_{\text{DLA}} - z_{\text{metal}}) \lesssim +0.07$.

4.2. $z_{\text{IGM,u}}$ versus z_{metal}

We should set $z_{\text{IGM,u}} = z_{\text{host}}$ if the GRB occurred in a galaxy embedded in the IGM that had not been ionized by the emission from the galaxy. Barkana & Loeb (2004) estimated that typical $z \sim 7$ GRBs occur in galaxies whose dark halo mass is $M_h \sim 4 \times 10^8 M_{\odot}$, based on the standard structure formation theory. They found that the proper (i.e., not comoving) radius of the ionized bubble created by stellar radiation from such galaxies would be $\lesssim 0.1$ Mpc, corresponding to a wavelength shift of $\Delta\lambda_{\text{obs}} \sim 3\text{\AA}$ or $(z_{\text{IGM,u}} - z_{\text{host}}) \sim -0.0025$. Instead, infall of IGM into the host galaxy may result in a relative redshift of the IGM absorption, with a wavelength shift of $\Delta\lambda_{\text{obs}} \lesssim 1\text{\AA}$ for a typical GRB host galaxy (Barkana & Loeb 2004). Since these are sufficiently small compared with the wavelength range of the damping wing, we set $z_{\text{IGM,u}} = z_{\text{host}}$ in the baseline model. On the other hand, Haiman (2002) estimated the proper size of ionized bubbles around LAEs detected in deep surveys as ~ 0.8 Mpc ($z_{\text{IGM,u}} - z_{\text{host}} \sim -0.02$), assuming a star formation rate (SFR) of $\sim 10 M_{\odot}/\text{yr}$ (as typically estimated for LAEs from the Ly α emission luminosity) and stellar age of 10^8 yr. This means a stellar mass greater than $M_* \sim 10^9 M_{\odot}$, which is considerably larger than that estimated by Barkana & Loeb (2004). Hence we consider that such a large ionized bubble is rather unlikely for *typical* GRBs at $z \sim 7$. It should be noted that the LAEs found in deep surveys are not necessarily typical galaxies or a tracer of typical star formation at $z \sim 7$.

Based on these considerations combined with the pos-

² This column density is slightly different from $\log N_{\text{HI}} = 21.3$ adopted in Paper I, which is the best-fit DLA model when z_{DLA} is treated as a free parameter (see §5.2). The following metallicity estimates are correspondingly different from those in Paper I, but the difference of this magnitude does not affect the arguments in this paper.

sible difference of z_{host} from z_{metal} discussed in §4.1, we define the possible range of $z_{\text{IGM,u}}$ as $-0.02 \lesssim (z_{\text{IGM,u}} - z_{\text{metal}}) \lesssim +0.07$, with a canonical value of $z_{\text{IGM,u}} = z_{\text{metal}}$.

5. Fitting to the Red Damping Wing

5.1. Fitting Procedures

In this section we will fit the models described above to the observed shape of the red damping wing. The fit is performed in a wavelength range of $\lambda_{\text{obs}} = 8925\text{--}9938\text{\AA}$. The lower bound corresponds to the wavelength where the wing drops sharply to the flux zero level. The wavelengths shorter than this are excluded since the noise by atmospheric lines is relatively high and there may be Ly α emission from the host galaxy (see discussion in §7.2). We then excluded the following wavelength regions of known absorption lines: 9033–9046 \AA (likely to be C IV in an intervening system at $z = 4.840$), 9137–9158 \AA (S II $\lambda 1253.8$), 9180–9206 \AA (S II $\lambda 1259.5$ + Si II $\lambda 1260.4$), 9218–9238 \AA (Si II* $\lambda 1264.7$), 9490–9505 \AA (O I $\lambda 1302.1$), and 9728–9750 \AA (C II $\lambda 1334.5$). In addition, we excluded a range of 9305–9490 \AA , since there are some absorption features that are probably atmospheric. There are 268 data points (pixels) in the final wavelength ranges used in the χ^2 analyses, which are indicated by thick horizontal lines in Fig. 1.

Then the model spectrum is fit to the data, with normalization always chosen to minimize the χ^2 value. In addition to the DLA and IGM absorptions, the Galactic extinction by $E(B - V) = 0.060$ mag (Schlegel, Finkbeiner, & Davis 1998) is also taken into account in the model spectrum. The spectral resolution is sufficiently narrower than the observed damping wing shape, and hence we ignore the smoothing effect by it. Figure 3 shows the histogram of the deviation of the data flux in a pixel from the model flux, $(F_{\text{data}} - F_{\text{model}})/F_{\text{error}}$, for one of the acceptable fits with $z_{\text{DLA}} = 6.295$, $\log N_{\text{HI}} = 21.62$, and $x_{\text{HI}} = 0$ ($\chi^2 = 277.29$). The distribution can well be fit by the Gaussian distribution, indicating that the error is well controlled and we can derive a reasonable statistical constraint on the model parameters by the standard χ^2 analyses.

5.2. Separate Fittings by DLA and IGM Absorption

As the first simple analysis, we try to fit the two components separately to the data. Figure 4 shows the confidence region of $N_{\text{HI}}\text{--}z_{\text{DLA}}$ for the DLA fit and $x_{\text{HI}}\text{--}z_{\text{IGM,u}}$ for the IGM fit. The best fits are $(\log N_{\text{HI}}, z_{\text{DLA}}) = (21.34, 6.320)$ with $\chi^2 = 265.54$ and $(x_{\text{HI}}, z_{\text{IGM,u}}) = (1.58, 6.348)$ with $\chi^2 = 270.79$, respectively.

The best-fit value of z_{DLA} is different from z_{metal} by $\sim +0.025$, which is considerably larger than that expected from the circular velocity of the host galaxy, indicating a possibility that the metal absorption system was accelerated by the GRB or its progenitor. However, $z_{\text{DLA}} = z_{\text{metal}} = 6.295$ is also marginally consistent within the confidence region of 99.7% C.L., and taking into account the arguments given in §4.1, we keep this case as the baseline model.

Interestingly, almost neutral IGM with $x_{\text{HI}} \sim 1$ extending to $z_{\text{IGM,u}} \sim 6.36$ gives a marginally acceptable fit for the red damping wing, indicating a possibility that we may have observed for the first time the signature of the completely neutral IGM before the reionization. The redshift difference of $(z_{\text{IGM,u}} - z_{\text{metal}}) \sim +0.065$ is within the theoretically possible range discussed in §4.2.

We show the model spectra for the two representative cases: “the DLA-dominated model” with $z_{\text{DLA}} = 6.295$ and $(\log N_{\text{HI}}, z_{\text{IGM,u}}, x_{\text{HI}}) = (21.62, 6.295, 0)$ in Fig. 1 and “the IGM-dominated model” with $(-\infty, 6.36, 1.0)$ in Fig. 2. Although the red damping wing shape can be reproduced even with $x_{\text{HI}} = 0$ in the DLA-dominated model, the IGM absorption with $x_{\text{HI}} \gtrsim 10^{-3}$ and $z_{\text{IGM,u}} \gtrsim 6.26$ are required for the absorption of photons blueward of the Ly α resonance.

5.3. DLA-IGM Joint Fitting

Next we try a joint fit including both the DLA and IGM absorptions. Here we treat $z_{\text{IGM,u}}$ as a free parameter but assume $z_{\text{DLA}} = z_{\text{metal}} = 6.295$ to reduce the number of free parameters. Figure 5 shows the allowed region for N_{HI} and x_{HI} , for several values of $z_{\text{IGM,u}}$. The best-fit is obtained at $(z_{\text{IGM,u}}, \log N_{\text{HI}}, x_{\text{HI}}) = (6.36, 21.59, 0.016)$ with $\chi^2 = 269.70$. Constraining $x_{\text{HI}} \geq 10^{-3}$ as inferred from the GP trough in quasar spectra at $z \gtrsim 6$, we obtain an upper limit of $z_{\text{IGM,u}} \leq 6.371$ at 99% C.L., otherwise the IGM absorption will erase the light transmission at $\lambda_{\text{obs}} \gtrsim 8950$ \AA .

As expected from the single component fits, the damping wing can be explained mostly by the DLA absorption at $z_{\text{DLA}} = 6.295$ with negligible IGM absorption, while it can also be fit dominantly by the IGM absorption with $x_{\text{HI}} \sim 1$ and $z_{\text{IGM,u}} \sim 6.36$. These results tell us that there is an unfavorable degeneracy between absorptions by a DLA and IGM (Miralda-Escudé 1998; Barkana & Loeb 2004). However, in the next section we show that this degeneracy can be broken by utilizing the features around the Ly β resonance.

5.4. Constraints from the Ly β Feature

Here we apply the same absorption models of the DLA and IGM, but for the Ly β transition at the restframe wavelength of $\lambda_{\beta} = 1025.72$ \AA . We use the same formulae given in §3, but replace λ_{α} and f_{α} by the corresponding values for Ly β . The Ly β absorption oscillator strength is $f_{\beta} = 0.07910$ and $g_u/g_l = 3$ is the same for all the Lyman series transitions by the selection rules (Cox 2000; Morton 1991). The frequency-integrated cross section $\int \sigma(\nu) d\nu$ is reduced by $f_{\beta}/f_{\alpha} = 0.190$, and the width of the damping wing in the wavelength space ($\propto \Lambda_{\beta} \lambda_{\beta}^2$) is reduced by the same factor. The optical depth of the red damping wing (τ_{IGM}) is reduced by a factor of $(f_{\beta}/f_{\alpha})^2 = 0.0361$ for the same z_{obs} ($= \lambda_{\text{obs}}/\lambda_{\beta} - 1$ for Ly β).

The predictions for the Ly β absorption feature are presented correspondingly to Ly α in Fig. 2. The feature of the DLA-dominated model is in good agreement with the data, while the emission (or, residual of absorption) feature around 7500–7520 \AA is clearly inconsistent

with the IGM-dominated model, in which the transmission is completely attenuated at wavelengths blueward of $\lambda_{\beta}(1 + z_{\text{IGM,u}}) \sim 7550\text{\AA}$. By visual inspection of the original CCD image of the spectrum (shown in Fig. 2), we confirmed that the feature of 7500–7520 \AA is the real signal. Therefore the Ly β feature safely excludes the IGM-dominated model. By requiring that the IGM Ly β absorption does not erase the feature at 7500–7520 \AA , we set a firm upper limit of $z_{\text{IGM,u}} \leq 6.314$, and within this constraint, the IGM absorption has only small contribution to the observed red damping wing even if $x_{\text{HI}} = 1$ (see dashed curves of Fig. 2). However, this contribution is not negligible, and in fact we can derive some constraint on x_{HI} , as will be shown below.

6. Implications for the IGM Neutral Fraction around GRB 050904

After the long analyses presented above, we finally arrived at the most likely interpretation of the red damping wing: it is mainly contributed by the DLA associated with the metal absorption lines at $z_{\text{metal}} = 6.295$, and the contribution from neutral IGM is not necessary at all. However, as shown in Fig. 2, if the IGM is completely neutral, the IGM absorption with $z_{\text{IGM,u}} \sim 6.295$ has small but non-negligible contribution to the observed damping wing shape. Then the next question is which value of x_{HI} is favored, under the constraints of $z_{\text{IGM,u}} = z_{\text{DLA}} = 6.295$ but N_{HI} is treated as an unknown free parameter and always chosen to minimize χ^2 for each value of x_{HI} .

For parameters other than x_{HI} and N_{HI} , we take $z_{\text{IGM,u}} = z_{\text{DLA}} = 6.295$, $z_{\text{IGM,l}} = 6$, $\beta_0 = -1.25$, and $A_V = 0$ as the baseline model parameters. We then find that χ^2 becomes minimum at $x_{\text{HI}} = 0$ with $\log N_{\text{HI}} = 21.62$, and it continuously increases with x_{HI} , changing the best-fit value of $\log N_{\text{HI}}$ to 21.54 at $x_{\text{HI}} = 1$. [The preference to smaller x_{HI} for $z_{\text{IGM,u}} \lesssim 6.32$ was also found in the results of the DLA-IGM joint fit (see §5.3 and Fig. 5).] Then formally we can estimate the confidence region of x_{HI} by requiring that $\Delta\chi^2(x_{\text{HI}}) \equiv \chi^2(x_{\text{HI}}) - \chi_{\text{min}}^2$ obeys the chi-square distribution with one degree of freedom (Lampton, Margon, & Bowyer 1976; Press et al. 1992). Table 1 presents the χ^2 values, the exclusion confidence level of the $x_{\text{HI}} = 1$ model corresponding to $\Delta\chi^2(1)$, and upper limits on x_{HI} with 68 (1 σ), 95, and 99 % C.L. We find the best fit value of $x_{\text{HI}} = 0.00$ in all models and upper limits of $x_{\text{HI}} < 0.17$ and 0.60 (68 and 95% C.L., respectively) for the baseline model.

In order to show why the $x_{\text{HI}} = 1$ model gives a worse fit, we plot in Fig. 6 the model spectra and the observed data in the form of the residual from the best-fit model of $x_{\text{HI}} = 0$ (the DLA-dominated model). The worse fit of the $x_{\text{HI}} = 1$ model comes from the combination of the two effects: the change of the damping wing shape in $\lambda_{\text{obs}} = 8900\text{--}9200\text{\AA}$ is not favored from the data, and the model predicts higher flux than the $x_{\text{HI}} = 0$ model at the longest wavelength range of $\lambda_{\text{obs}} \gtrsim 9500\text{\AA}$, while the data favor even lower flux than that of the $x_{\text{HI}} = 0$ model.

Before we conclude that the case of $x_{\text{HI}} = 1$ is not fa-

vored, however, any systematic uncertainties must be explored. The results of this uncertainty check will be given below. Table 1 shows the fit results changing one or two of the model parameters while the other parameters are kept to the values of the baseline model. (The DLA column density N_{HI} is treated always as a free parameter minimizing χ^2 .) We found that the χ^2 is minimized at $x_{\text{HI}} = 0$ in all cases, favoring smaller values.

6.1. Spectral Index of the Afterglow SED

The change of the afterglow spectral index, β_0 , within the quoted error of $\Delta\beta_{\text{obs}} = \pm 0.25$ (Tagliaferri et al. 2005) does not have a significant effect. As can be seen in Fig. 6, the data favors a bluer spectrum than the baseline model with $\beta_0 = -1.25$, and hence a larger β_0 gives a better fit. However, this effect is not large; the change of $\Delta\beta_0 = 0.25$ in the wavelength range of 9000–10000 \AA results in the fractional change of $\sim 2.4\%$ in F_{λ} , or ~ 0.024 in Fig. 6. It should be noted that the quoted error of Haislip et al. (2005) is even smaller ($\Delta\beta_{\text{obs}} = {}^{+0.15}_{-0.14}$). If the cooling frequency break in the SED passed through the NIR bands at an epoch between the photometric observations and our spectroscopic observation, the afterglow SED would become even redder, which is not favored from our data.

6.2. Dust Extinction in the Host Galaxy

Though the observed NIR colors do not show evidence for extinction by dust in the host galaxy (Tagliaferri et al. 2005), the wavelength coverage by photometric observations redward of the Lyman break is rather narrow, and substantial extinction may still be possible. Therefore we tried a model with substantial extinction, where the original afterglow spectrum β_0 is chosen so that the expected NIR colors are consistent with the observed ones. The change of observed ($J - K$) color at $z \sim 6.3$ can be related to the restframe V magnitude extinction as $\Delta(J - K) = 0.68A_V$ and $1.83A_V$ for the extinction curves of the Milky Way (MW) and the SMC, respectively (e.g., Pei 1992). On the other hand, the change of the afterglow spectral index is related to the NIR color as $\Delta(J - K) = -0.61\Delta\beta_0$. Therefore the expected ($J - K$) color is not changed if we introduce extinction with changing β_0 by a relation, $A_V = 0.90\Delta\beta_0$ (MW) or $0.33\Delta\beta_0$ (SMC). In Table 1, we show the fit results by models with $A_V = 0.45$ (MW) and 0.17 (SMC) corresponding to $\Delta\beta_0 = +0.5$ ($\beta_0 = -0.75$). Here we have used the functional form of extinction $A(\lambda)$ around $\lambda \sim \lambda_{\alpha}$ given in Barkana & Loeb (2004). We found that both χ^2 and $\Delta\chi^2$ are increased by introducing extinction by dust, indicating that substantial extinction is not favored and does not change the preference to lower x_{HI} values.

6.3. The Redshift Parameters

Changing $z_{\text{IGM,u}}$ within the possible range of 6.27–6.314 does not change the preference to lower x_{HI} values. Because $z_{\text{IGM,l}}$ is rather uncertain, changing this parameter has a relatively large effect. Larger values of $z_{\text{IGM,l}}$ result in a smaller amount of the neutral IGM and hence the upper limit on x_{HI} becomes weaker. However, the

completely neutral IGM can still be excluded by $\sim 90\%$ C.L. even for $z_{\text{IGM},l} = 6.2$.

To show the characteristic redshift range of IGM neutral hydrogen contributing to τ_{IGM} , we plot τ_{IGM} as a function of $z_{\text{IGM},l}$ with $z_{\text{IGM},u} = 6.295$, for three values of $\lambda_{\text{obs}} = 8925$ (the lower bound of the wavelength range used in the fitting analysis), 8970, and 9050 Å, in Fig. 7. The IGM optical depth is shown as a ratio to that with $z_{\text{IGM},l} = 0$, which is $\tau_{\text{IGM}} = 0.37, 0.20,$ and 0.10 for the three values of λ_{obs} , respectively. From this figure we see that more than half and 80% of the IGM optical depth is contributed from hydrogens at $z \gtrsim 6.2$ and 6.0 , respectively.

As a check for the possibility that z_{DLA} is different from z_{metal} but $z_{\text{DLA}} = z_{\text{host}}$, we tested the models with $z_{\text{DLA}} = z_{\text{IGM},u} = 6.29$ and 6.314 . This range can be derived assuming $z_{\text{host}} = z_{\text{IGM},u}$ and taking into account the possible ranges of z_{host} and $z_{\text{IGM},u}$ with respect to z_{metal} , as well as the constraint from the transmission around the Ly β wavelength. We found that the preference to low x_{HI} is not changed.

6.4. Weak Unidentified Absorption Lines

It is difficult to quantitatively estimate the possible systematic effects by weak absorption lines that cannot be discriminated from noise. However, if such weak lines are distributed uniformly in the fitting wavelength range, the effect is simply changing the overall normalization that would not affect our conclusions. We also repeated the same calculation without removing the wavelength ranges of the identified absorption feature, to see the sensitivity to the absorption features (see the ‘‘Lines Included’’ row of Table 1). The data points are now 379, and χ^2 is unacceptably large due to the absorption features that are not included in the model. However, we find a similar $\Delta\chi^2(1)$, and hence the preference to small x_{HI} values is not sensitive to the treatment of absorption lines.

The absorption by vibrationally excited molecular hydrogen may affect the spectrum around the restframe Ly α (Draine 2000; Draine & Hao 2002). In fact, Haislip et al. (2006)³ proposed that the anomalously attenuated Z-band flux by a factor of ~ 3 of the early afterglow of GRB 050904 is due to the molecular hydrogen absorption. However, this signature completely disappeared by ~ 3 days, and hence it is unlikely to affect our spectrum taken 3.4 days after the burst. The molecular hydrogen signatures have not yet been clearly detected in other afterglow spectra (e.g., Schaefer et al. 2003; Vreeswijk et al. 2004).

6.5. Time Variability

Ionization by strong afterglow flux may result in the time variability of the amount of hydrogen and metal absorptions (Perna & Loeb 1998; Draine & Hao 2002). Though statistically significant variability was not found in the observed spectrum of GRB 050904, variability within the errors cannot be excluded. If such a variability of N_{HI} is present, the observed shape of the damping

wing is a superposition of the shapes with different values of N_{HI} . It may induce systematic bias in the analysis presented here, since the damping wing shape depends non-linearly on N_{HI} . As a test of this possibility, we tried an extreme model where the spectrum is a mean of the two spectra with different values of the column density, N_+ and N_- , as $\log N_{\pm} \equiv \log N_{\text{HI}} \pm \Delta \log N_{\text{HI}}$. We take $\Delta \log N_{\text{HI}} = 0.2$ as the variability allowed within the observational error, which is inferred from the statistical error of $\log N_{\text{HI}}$ obtained by the fitting analysis (see Fig. 4). We then find that the preference to lower x_{HI} is hardly changed even for this rather extreme model (see the ‘‘Variability Check’’ row of Table 1).

It should be noted that the neutral hydrogen shell must be very close to the burster, as $r \lesssim 4 \times 10^{17}$ cm, in order for the column density of $N_{\text{HI}} \sim 21.6$ to substantially change during the spectroscopic observation by the ionizing flux estimated from the observed F_{λ} . This scale is close to the location of the external shock at 3.4 days in observer’s time for typical afterglow parameters and $z = 6.3$ (e.g., Sari, Piran, & Narayan 1998). We derived in Paper I an estimate of electron density $n_e \sim 10^{2.3 \pm 0.7} \text{ cm}^{-3}$ from the observed fine-structure Si^{II*} line, assuming collisional excitation by electrons. The ionization fraction is unknown, and if ionization fraction is much smaller as $n_e/n_H \lesssim 10^{-4}$, the excitation by neutral hydrogen becomes more important, leading to a density estimate of $n_H \sim 10^4 \text{ cm}^{-3}$ (Silva & Viegas 2002). Combined with the DLA column density, the DLA scale of $\sim 0.1\text{--}1$ pc is inferred. On the other hand, Berger et al. (2005b) suggested a possibility of fine-structure excitation by GRB afterglow radiation for the case of GRB 051111, deriving a larger distance scale of $\sim 10\text{--}20$ pc. Therefore the scale estimate is rather uncertain, but it seems that there is a parameter space of the DLA where no N_{HI} variability is expected but it is close enough to be consistent with the Si^{II*} detection.

Based on these results, we conclude that there is an evidence for considerable ionization of the IGM around the host galaxy of GRB 050904 already at $z = 6.3$.

7. Discussion

7.1. Prediction for the Case of Low N_{HI}

We found that the DLA column density is $\log N_{\text{HI}} \gtrsim 21$ for GRB 050904, and in such a case the DLA absorption dominates the absorption by neutral IGM extending to the same redshift as that of the DLA. Therefore it is difficult to derive a very strong constraint on x_{HI} , though we obtained some constraints as presented above by detailed statistical analyses. Vreeswijk et al. (2004) compiled seven GRBs having estimates of N_{HI} from afterglow spectra, and though the majority of them have column densities larger than $\log N_{\text{HI}} \geq 21$, two (GRB 011211 and GRB 021004) have low column densities of $\log N_{\text{HI}} \lesssim 20$. If we detect such a GRB at $z \gtrsim 6$, it would provide an opportunity to probe the reionization with a much cleaner environment.

To demonstrate this possibility, we show a model with $(\log N_{\text{HI}}, x_{\text{HI}}) = (20.0, 1.0)$ with $z_{\text{DLA}} = z_{\text{IGM},u} = z_{\text{metal}} =$

³ In their e-print version (astro-ph/0509660).

6.295, in Fig. 8. In this case the shape of the damping wing is dominantly contributed by the neutral IGM absorption. Also shown is DLA absorption at the same redshift but with various values of N_{HI} . It can be seen that the shape of IGM absorption is different from that of DLAs with any values of N_{HI} , making it possible to prove the dominance of the IGM component. Another possibility to explain such a data by DLA absorption is to consider a blueshifted absorption by a DLA with a relative velocity of a few thousands km/s with respect to z_{metal} , as we observed the degeneracy between the DLA and IGM absorptions in §5.2. Such a velocity may again be achieved by acceleration of absorbing clouds by the activity of GRBs or their progenitors, but such absorbers are likely to be polluted by metals, and we expect blueshifted metal lines as well, in addition to those in the restframe of the host galaxy. Therefore we can discriminate this case as well, and hence high-quality spectra of low- N_{HI} afterglows in the future will provide us with an invaluable opportunity to measure x_{HI} more accurately.

7.2. Ly α Emission from Host Galaxies and Reionization

We expect Ly α emission in the spectrum, if the huge HI absorption is by gas in the vicinity of the GRB and the host galaxy has detectable Ly α emission like GRB 030323 (Vreeswijk et al. 2004). The spectrum of GRB 050904 does not show a clear Ly α emission (§2) and we set an upper limit on the Ly α flux of $F(\text{Ly}\alpha) < 1.7 \times 10^{-18} \text{ erg cm}^{-2}\text{s}^{-1}$ for a width of 8.5 Å, which is the FWHM of the spectral resolution and corresponding to a velocity dispersion of ~ 300 km/s as well. Then the upper bound on the Ly α luminosity becomes $L(\text{Ly}\alpha) < 7.9 \times 10^{41} \text{ erg/s}$ at $z = 6.295$, which can be translated into extinction-uncorrected SFR of $< 0.79 M_{\odot}/\text{yr}$, by using the empirical relation (Kennicutt 1998; Cowie & Hu 1998).

It has been indicated that the Ly α emission from GRB host galaxies is stronger in terms of the equivalent width (EW) than that from Lyman-break galaxies (LBGs) at similar redshift ($z \sim 3$); all GRB host galaxies at $z \gtrsim 2$ are consistent with having $\text{EW}_{\text{rest}}(\text{Ly}\alpha) > 10 \text{ \AA}$ (Fynbo et al. 2003; Jakobsson et al. 2005), which is as large as that of LAEs found in deep surveys. For comparison, only about a third of LBGs at similar redshifts have such large EW (Shapley et al. 2003). Then it is suggested that Ly α emission from host galaxies of GRBs at $z \gtrsim 6$ may also give some information on the reionization.

To demonstrate this possibility, we show the IGM absorption profile with $z_{\text{IGM,u}} = 6.295$ for $x_{\text{HI}} = 0.01, 0.2$, and 1.0 in Fig. 2. If $x_{\text{HI}} \sim 1$ and the Ly α line center is the same as $\lambda_{\alpha}(1 + z_{\text{IGM,u}})$, the Ly α photons within $\sim 10 \text{ \AA}$ from the line center are heavily absorbed. For comparison, LAEs detected at $z \sim 6$ show line widths of $\sim 10 \text{ \AA}$, corresponding to a few hundreds km/s (Kodaira et al. 2003; Taniguchi et al. 2005). Even larger velocity dispersion may also be possible; a redward tail of Ly α emission extending beyond a relative velocity difference of $\gtrsim 1000$ km/s has been found in a starburst galaxy at $z \sim 3$ (Pettini et al. 2000). Then we expect that, if $x_{\text{HI}} \sim 1$, the Ly α line luminosity is strongly attenuated allowing transmission only in the

redward tail. On the other hand, if $x_{\text{HI}} \lesssim 0.01$, about half of the Ly α emission is transmitted. Therefore statistical comparison of Ly α line emissivity of GRB host galaxies at $z \gtrsim 6$ and $\lesssim 6$ may give an interesting information for the reionization.

As a reionization probe based on Ly α emission, GRB host galaxies have an advantage of no selection effect compared with LAEs selected by Ly α emission. Brightness of afterglows allows us to accurately measure the redshift by metal absorption lines, as demonstrated by GRB 050904, and hence the plausible Ly α line center can be determined more accurately than LAEs or LBGs. It should be noted that, even though LAEs at $z \sim 6$ have asymmetric Ly α emission profiles with a sharp cut-off at the blueward side, a strong conclusion about the IGM neutral fraction cannot be derived because of the general lack of information about the line center (Haiman 2002). On the other hand, since the brightness of host galaxies is not relevant to the detectability of GRBs, typical GRBs may occur in smaller galaxies than LAEs/LBGs, and hence typical absolute Ly α luminosity may be smaller, in spite of the suggestion of large EW for GRB host galaxies. (See §4.2 for a discussion about the typical mass of GRB host galaxies at $z \sim 6$ expected from the structure formation theory.) A larger sample of GRB host galaxies at $z \gtrsim 6$ is necessary to investigate more about these possibilities.

Concerning the case of GRB 050904, a search for the host galaxy in the z' band will be interesting in this context. Assuming $\text{EW}_{\text{rest}}(\text{Ly}\alpha) \geq 10 \text{ \AA}$ as suggested for GRB host galaxies, the obtained upper bound on Ly α emission requires that the continuum level of the host galaxy must be lower than $F_{\lambda} \leq 2.3 \times 10^{-20} (\text{EW}_{\text{rest}}/10 \text{ \AA})^{-1} \text{ erg cm}^{-2}\text{s}^{-1}\text{\AA}^{-1}$. Since the Lyman break is in the midst of the z' band filter, we take into account a dimming by a factor of about 2, and we get the corresponding AB magnitude of $z' > 27.7$. Therefore, if follow-up observations find the host galaxy of GRB 050904 brighter than $z' = 27.7$, it would mean that $\text{EW}_{\text{rest}}(\text{Ly}\alpha) < 10 \text{ \AA}$, which is smaller than those found in GRB host galaxies at $z \sim 3$. Thus it indicates a possibility of attenuation by neutral IGM, though only one case is not sufficient and statistical studies are required. Galaxies brighter than $z' = 27.7$ can be detected by imaging observations of existing large telescopes; typical magnitude of LAEs at $z \sim 6.6$ found in the Subaru Deep Field is $z' \sim 26\text{--}27.8$ (Taniguchi et al. 2005).

8. Summary and Conclusions

We presented a comprehensive theoretical modeling of the red damping wing of the Ly α absorption found in the optical afterglow spectrum of GRB 050904 at $z \sim 6.3$, which provides the first opportunity of studying the cosmic reionization by using GRBs. We tried to model the observed damping wing shape by the two components of absorbers: one is by the DLA associated to the GRB host galaxy, and the other is by neutral hydrogen in the IGM. The redshift of the metal absorption lines in the spectrum is $z_{\text{metal}} = 6.295 \pm 0.002$, but we allowed different values of

z_{DLA} (the DLA redshift) and $z_{\text{IGM,u}}$ (the upper extension bound of neutral hydrogens in the IGM), and discussed various theoretical possibilities for the deviation of these parameters from z_{metal} .

The shape of the red damping wing can be explained either by the DLA at $z_{\text{DLA}} \sim z_{\text{metal}}$ with $\log N_{\text{HI}} \sim 21.6$, or by almost neutral IGM extending to a higher redshift of $z_{\text{IGM,u}} \sim 6.36$. Though the DLA seems a more straightforward interpretation, we cannot exclude the latter possibility simply by the redshift difference, since blueshift of metal absorption lines up to a few thousands km/s with respect to the restframe of the host galaxy has been observed in a few GRBs.

However, we found that the Ly β feature can be used to break this degeneracy, since the two different solutions predict different wavelengths at which the Ly β GP trough ends. Then we concluded that the damping wing is mostly contributed from the DLA at $z_{\text{DLA}} \sim z_{\text{metal}}$, and derived a firm upper bound of $z_{\text{IGM,u}} \leq 6.314$. We argued that the DLA is likely to be associated physically with the metal absorption lines, and the inferred column densities, metallicities, and depletion of silicon are all reasonable as a DLA found in a GRB afterglow.

Next we examined the preferred value of the IGM neutral fraction, x_{HI} , in the viable model of $z_{\text{IGM,u}} = z_{\text{DLA}} = 6.295$. Treating N_{HI} of the DLA as a free parameter, we found that a smaller value of x_{HI} is favored with the best-fit value of $x_{\text{HI}} = 0.00$, and upper limits of $x_{\text{HI}} < 0.17$ and 0.60 (68 and 95% C.L., respectively) were derived. We examined various possible systematic uncertainties that could affect this result, including the afterglow spectral index, dust extinction at the host galaxy, the redshift parameters of the DLA and IGM absorptions, weak unidentified absorption lines, and time variability of the DLA column density. We found that none of these effects is large enough to change the above result. Hence we conclude that the universe was largely ionized already at $z \sim 6.3$, excluding the completely neutral IGM at $\sim 99\%$ C.L.

This is the first quantitative *upper* limit on x_{HI} at $z \gtrsim 6$ by a direct method,⁴ being consistent with the recent results by an indirect approach using the number density evolution of LAEs (Malhotra & Rhoads 2004; Stern et al. 2005; Haiman & Cen 2005). Since the IGM is optically thin for photons in the damping wing region, all the IGM neutral hydrogens at $z \sim 6.1$ – 6.3 (see Fig. 7) contribute to the damping wing, allowing us to derive a robust constraint on the mass-weighted x_{HI} which is insensitive to any clumpiness of IGM within this redshift interval. Combined with the suggestions of $x_{\text{HI}} \gtrsim 0.1$ from quasar spectra (Mesinger & Haiman 2004; Wyithe, Loeb, & Carilli 2005), a plausible value of $x_{\text{HI}} \sim 0.1$ is suggested for the IGM at $z \sim 6$ – 6.3 .

⁴ Though there are some “data points” of the IGM optical depth at $z \gtrsim 6$ derived directly from the GP trough of quasar spectra (Fan et al. 2006), these are by averaging sharp spikes of transmission in a wavelength range, which are probably corresponding to small regions of ionized bubbles. Therefore there is no upper limit on the mass-weighted or volume-weighted optical depth.

The large DLA column density of $\log N_{\text{HI}} \gtrsim 21$ dominates the IGM absorption extending to the same redshift, making it difficult to derive a stronger constraint on x_{HI} than derived here. However, some GRBs have low column densities of $\log N_{\text{HI}} \lesssim 20$, and detection of such GRBs at $z \gtrsim 6$ will be a promising chance to get better information for the reionization history of the universe.

We did not detect Ly α emission from the host galaxy, leading to an upper limit for extinction-uncorrected star formation rate as $\text{SFR} \lesssim 0.79 M_{\odot}/\text{yr}$. We discussed the potential of Ly α emission from GRB host galaxies as a reionization probe. Statistically smaller equivalent width and transmission only at the red tail of Ly α emission are expected for GRB host galaxies before the reionization, compared with those at lower redshifts. This may be tested by using future large samples of GRBs at $z \gtrsim 6$. As a reionization probe using Ly α emission, GRB host galaxies have an advantage of being free from the selection bias compared with LAEs. Another advantage compared with both LAEs and LBGs is that an accurate redshift determination is possible by absorption lines in bright afterglows. On the other hand, a possible disadvantage is that typical GRB host galaxies and their absolute Ly α luminosity may not be as bright as LAEs and LBGs found in deep surveys.

We conclude that the GRB 050904 has opened a new era of cosmological study by GRBs, and future data will give us even more unique and important information about the epoch when the early-generation luminous objects changed the physical state of almost all the baryonic matter in the cosmos.

We would like to thank the Subaru Telescope staff for their warm assistance in taking this invaluable data. We would also like to thank the referee for useful comments. This work was supported in part by the Grant-in-Aid for the 21st Century COE “Center for Diversity and Universality in Physics” from the Ministry of Education, Culture, Sports, Science, and Technology (MEXT) of Japan. T.T. and N.K. were also supported by the Grant-in-Aid for Scientific Research from the MEXT, 16740109 and 14GS0211, respectively.

References

- Andersen, M.I., et al. 2000, *A&A*, 364, L54
- Ando, M., Ohta, K., Iwata, I. Watanabe, C., Tamura, N., Akiyama, M., & Aoki, K. 2004, *ApJ*, 610, 635
- Bajtlik, S., Duncan, R.C., & Ostriker, J.P. 1988, *ApJ*, 327, 570
- Barkana, R. & Loeb, A. 2001, *Phys. Rep.* 349, 125
- Barkana, R. & Loeb, A. 2004, *ApJ*, 601, 64
- Barth, A.J. et al. 2003, *ApJ*, 584, L47
- Becker, R.H. et al. 2001, *AJ*, 122, 2850
- Berger, E., Penprase, B.E., Cenko, S.B., Kulkarni, S.R., Fox, D.B., Steidel, C.C., & Reddy, N.A. 2005a, submitted to *ApJ*, astro-ph/0511498
- Berger, E., Penprase, B.E., Fox, D.B., Kulkarni, S.R., Hill, G., Schaefer, B., & Reed, M. 2005b, submitted to *ApJL*, astro-ph/0512280
- Boër, M., Atteia, J.-L., Damerdji, Y., Gendre, B., Klots, A., & Stratta, G. 2005, submitted to *Nature*, astro-ph/0510381

- Bouchet, P., Lequeux, J., Maurice, E., Prevot, L., & Prevot-Burnichon, M. L. 1985, *A&A*, 149, 330
- Bouwens, R. J., et al. 2004, *ApJ*, 606, L25
- Cen, R. & Haiman, Z. 2000, *ApJ*, 542, L75
- Cen, R. & McDonald, P. 2002, *ApJ*, 570, 457
- Cen, R. 2003, *ApJ*, 591, 12
- Chen, H.-W., Prochaska, J.X., Bloom, J.S., & Thompson, I.B. 2005, to appear in *ApJL*, astro-ph/0508270
- Ciardi, B. & Loeb, A. 2000, *ApJ*, 540, 687
- Cowie, L.L. & Hu, E. M. 1998, *AJ*, 115, 1319
- Cox, A.N. 2000, *Allen's Astrophysical Quantities*, 4th ed. (Springer-Verlag: New York)
- Cusumano, G. et al. 2005, *Nature* 440, 164
- De Pasquale, M. et al. 2005, to appear in *MNRAS*, astro-ph/0510566
- Dickinson, M., et al. 2004, *ApJ*, 600, L99
- Djorgovski, S.G., Castro, S.M., Stern, D., Mahabal, A.A. 2001, *ApJ*, 560, 5
- Draine, B.T. 2000, *ApJ*, 532, 273
- Draine, B.T. & Hao, L. 2002, *ApJ*, 569..780
- Fan, X. et al. 2002, *AJ*, 123, 1247
- Fan, X. et al. 2003, *AJ*, 125, 1649
- Fan, X. et al. 2006, *AJ* submitted, astro-ph/0512082
- Fruchter, A., Krolik, J.H. & Rhoads, J.E. 2001, *ApJ*, 563, 597
- Fynbo, J.P.U. et al. 2001, in the proceedings of "Lighthouses of the Universe" in Garching (Germany), August 2001 (astro-ph/0110603)
- Fynbo, J.P.U. et al. 2003, *A&A*, 406, L63
- Galama, T. & Wijers, R.A.M.J. 2001, *ApJ*, 549, L209
- Giavalisco, M., et al. 2004, *ApJ*, 600, L103
- Gresse, N. & Sauval, A.J. 1998, *Space Sci. Rev.* 85, 161
- Gunn, J.E. & Peterson, B.A. 1965, *ApJ*, 142, 1633
- Haiman, Z. 2002, *ApJ*, 576, L1
- Haiman, Z. 2004, in *Carnegie Observatories Astrophysics Series*, Vol. 1, *Coevolution of Black Holes and Galaxies*, ed. L. C. Ho (Cambridge: Cambridge Univ. Press), 67
- Haiman, Z. & Cen, R. 2005, *ApJ*, 623, 627
- Haislip, J. B. et al. 2006, *Nature* 440, 181
- Hjorth, J. et al. 2003a, *Nature*, 423, 847
- Hjorth, J. et al. 2003b, *ApJ*, 597 699
- Hu, E. et al. 2002, *ApJ*, 568, L75
- Iye, M. et al. 2004, *PASJ*, 56, 381
- Jakobsson, P. et al. 2005, *MNRAS*, 362, 245
- Jensen, B.L. et al. 2001, *A&A*, 370, 909
- Kashikawa, N. et al. 2002, *PASJ*, 54, 819
- Kawai, N. et al. 2006, *Nature* 440, 184 (Paper I)
- Kawasaki, M., Kohri, K., & Moroi, T. 2005, *Phys. Rev. D* 71, 083502
- Kennicutt, R.C. 1998, *ARA&A*, 36, 189
- Klebesadel, R.W., Strong, I.B., & Olson, R.A. 1973, *ApJ*, 182, L85
- Klose, S. et al. 2004, *AJ*, 128, 1942
- Kodaira, K. et al. 2003, *PASJ*, 55, L17
- Kogut, A. et al. 2003, *ApJS*, 148, 161
- Kulkarni, S. et al. 1998, *Nature*, 393, 35
- Kulkarni, S. et al. 1999, *Nature*, 398, 389
- Lamb, D.Q. & Reichart, D.E. 2000, *ApJ*, 536, 1
- Lampton, M., Margon, B., & Bowyer, S. 1976, *ApJ*, 208, 177
- Larson, R.B. 1981, *MNRAS*, 194, 809
- Loeb, A. & Barkana, R. 2001, *ARA&A*, 39, 19
- Madau, P. & Rees, M.J. 2000, *ApJ*, 542, L69
- Malhotra, S. & Rhoads, J. 2004, *ApJ* 617, L5
- Mesinger, A. & Haiman, Z. 2004, *ApJ*, 611, 69
- Mészáros, P. 2002, *ARA&A*, 40, 137
- Metzger, M. R., Djorgovski, S. G., Kulkarni, S. R., Steidel, C. C., Adelberger, K. L., Frail, D. A., Costa, E., & Frontera, F. 1997, *Nature*, 387, 879
- Mirabal, N. et al. 2003, *ApJ*, 595, 935
- Miralda-Escudé, J. 1998, *ApJ*, 501, 15
- Miralda-Escudé, J. 2003, *Science*, 300, 1904
- Møller, P. et al. 2002, *A&A*, 396, L21
- Morton, D.C. 1991, *ApJS*, 77, 119
- Peebles, P.J.E. 1993, *Principles of Physical Cosmology* (Princeton: Princeton Univ. Press)
- Pei, Y.C. 1992, *ApJ*, 395, 130
- Perna, R. & Loeb, A. 1998, *ApJ*, 501, 467
- Pettini, M., Steidel, C.C., Adelberger, K.L., Dickinson, M., & Giavalisco, M. 2000, *ApJ*, 528, 96
- Piran, T. 2004, *Rev. Mod. Phys.* 76, 1143
- Predehl, P. & Schmitt, J.H.M.M. 1995, *A&A*, 293, 889
- Press, W.H., Teukolsky, S.A., Vetterling, W.T., & Flannery, B.P. 1992, *Numerical Recipes* (Cambridge, Cambridge), chapter 15
- Price, P.A., Cowie, L.L., Minezaki, T., Schmidt, B.P., Songaila, A., & Yoshii, Y. 2005, submitted to *ApJ Lett.*, astro-ph/0509697
- Prochaska, J.X., Gawiser, E.G., Wolfe, A.M., Castro, S. & Djorgovski, S.G. 2003, *ApJ*, 595, L9
- Sari, R., Piran, T., & Narayan, R. 1998, *ApJ*, 497, L17
- Savaglio, S., Fall, S.M., & Fiore, F. 2003, *ApJ*, 585, 638
- Savaglio, S. & Fall, S.M. 2004, *ApJ*, 614, 293
- Schaefer, B.E. et al. 2003, *ApJ*, 588, 387
- Schlegel, D.J., Finkbeiner, D.P., & Davis, M. 1998, *ApJ*, 500, 525
- Shapley, A.E., et al. 2003, *ApJ*, 588, 65
- Silva, A.I. & Viegas, S.M. 2002, *MNRAS*, 329, 135
- Solomon, P. M., Rivolo, A. R., Barrett, J., & Yahil, A. 1987, *ApJ*, 319, 730
- Songaila, A. & Cowie, L.L. 2002, *AJ*, 123, 2183
- Spergel, D.N. et al. 2003, *ApJS*, 148, 175
- Stanek, K.Z. et al. 2003, *ApJ*, 591, L17
- Stanway, E. R., et al. 2004, *ApJ*, 604, L13
- Starling, R.L.C. et al. 2005, to appear in *A&A*, astro-ph/0508237
- Stern, D. et al. 2005, *ApJ*, 619, 12
- Tagliaferri, G. et al. 2005, to appear in *A&A Lett.*, astro-ph/0509766
- Taniguchi, Y. et al. 2005, *PASJ*, 57, 165
- Totani, T. 1997, *ApJ*, 486, L71
- Viegas, S.M. 1995, *MNRAS*, 276, 268
- Vladilo, G., Centurión, M., Bonifacio, P., & Howk, J.C. 2001, *ApJ*, 557, 1007
- Vreeswijk, P.M. et al. 2004, *A&A*, 419, 927
- Vreeswijk, P.M. et al. 2005, *A&A* in press, astro-ph/0510404
- Watson, D. et al. 2005a, to appear in *ApJL*, astro-ph/0509640
- Watson, D. et al. 2005b, submitted to *ApJ*, astro-ph/0510368
- Waxman, E. & Draine, B.T. 2000, *ApJ*, 537, 796
- White, R.L., Becker, R.H., Fan, X., & Strauss, M. 2003, *ApJ*, 126, 1
- Wijers, R.A.M.J., Bloom, J.S., Bagla, J.S., & Natarajan, P. 1998, *MNRAS*, 294, L13
- Wyithe, J.S.B. & Loeb, A. 2003, *ApJ*, 586, 693
- Wyithe, J.S.B. & Loeb, A. 2004, *Nature*, 427, 815
- Wyithe, J.S.B. & Loeb, A. 2005, *ApJ*, 625, 1
- Wyithe, J.S.B., Loeb, A. & Carilli, C. 2005, *ApJ*, 628, 575

Table 1. Constraint on x_{HI} for Various Models

Models	$\chi^2_{\text{min}} \dagger$	$\chi^2(x_{\text{HI}} = 1)$	$\Delta\chi^2(x_{\text{HI}} = 1)$	C.L.(%) [‡]	upper limits on x_{HI}^*		
					68	95	99 C.L. (%)
Baseline [§]	277.29	284.12	6.84	99.1	0.17	0.60	0.98
$\beta_0 = -1/-1.5$	273.86/281.10	280.07/288.75	6.21/7.65	98.7/99.4	0.18/0.15	0.66/0.52	1.08/0.88
$A_V = 0.45/0.17^{\P}$	316.93/283.18	329.72/291.12	12.80/7.94	99.97/99.5	0.09/0.15	0.32/0.52	0.54/0.85
$z_{\text{IGM,u}} = 6.27/6.314$	277.29/277.29	283.55/283.21	6.27/5.93	98.8/98.5	0.19/0.19	0.63/0.68	1.06/1.12
$z_{\text{IGM,l}} = 5.5/6.2$	277.29/277.29	286.70/280.07	9.41/2.78	99.8/90.5	0.13/0.38	0.45/1.36	0.74/2.22
$z_{\text{DLA}} = 6.29/6.314^{\parallel}$	281.47/266.41	288.49/271.25	7.03/4.83	99.2/97.2	0.16/0.27	0.57/0.84	0.96/1.27
Lines Included	796.03	802.53	6.50	98.9	0.17	0.63	1.02
Variability Check	283.98	289.54	5.56	98.2	0.20	0.71	1.18

*See §3 for the reason why the apparently unphysical cases of $x_{\text{HI}} > 1$ are allowed here.

[†]In all models, χ^2 increases with x_{HI} and the minimum χ^2 is realized at $x_{\text{HI}} = 0$.

[‡]The exclusion confidence level for the case of $x_{\text{HI}} = 1$.

[§]The baseline model parameters are: $z_{\text{IGM,u}} = z_{\text{DLA}} = 6.295$, $z_{\text{IGM,l}} = 6$, $\beta_0 = -1.25$, and $A_V = 0$. The second row and below show the models when some parameters are changed from the baseline model.

[¶]The spectral index is changed into $\beta_0 = -0.75$ to keep the expected NIR colors consistent with the observed ones for the MW/SMC extinction curves, respectively.

^{||}The IGM redshift parameter $z_{\text{IGM,u}}$ is kept to be the same with z_{DLA} .

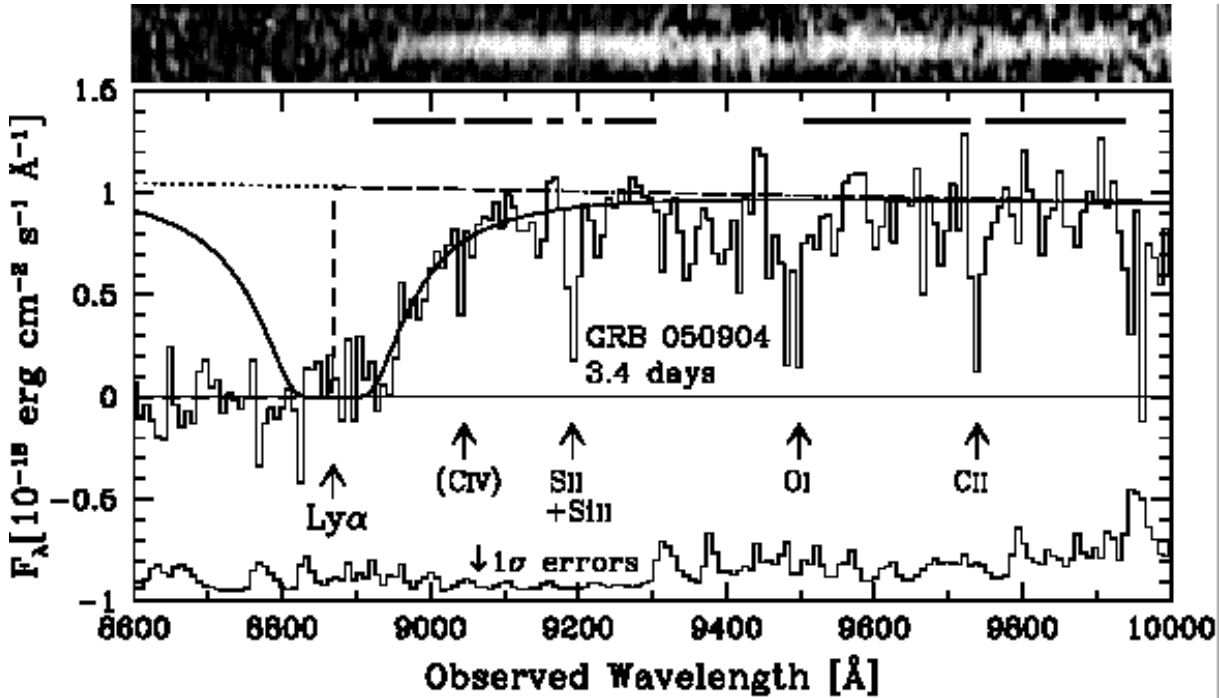


Fig. 1. The afterglow spectrum of GRB 050904 taken 3.4 days after the burst. The spectrum is binned by 3 pixels, and 1σ errors are also shown with an offset of -1.0 . The CCD image of the spectrum in the corresponding wavelength range is shown at the top of the figure. The $\text{Ly}\alpha$ resonance and identified absorption lines are indicated with the redshift $z_{\text{metal}} = 6.295$, except for the intervening CIV system at $z = 4.840$. The thick horizontal lines in the upper right region show the wavelength ranges used in the spectral fitting, where identified absorption features are removed. The solid curve shows the model absorption by a DLA with $\log N_{\text{HI}} = 21.62$ and $z_{\text{DLA}} = 6.295$ (the DLA-dominated model). The dotted line shows the original unabsorbed spectrum of the afterglow, with the spectral index of $\beta_0 = -1.25$. The dashed curve shows the model absorption by the IGM with $z_{\text{IGM,u}} = 6.295$ and $x_{\text{HI}} = 10^{-3}$, which is almost a vertical line at the $\text{Ly}\alpha$ resonance. The Galactic extinction of $E(B - V) = 0.060$ mag is taken into account in all the model curves.

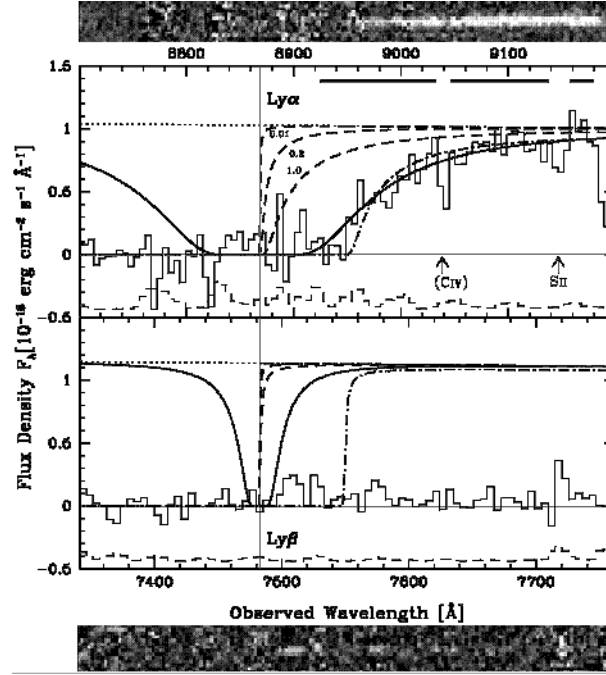


Fig. 2. The same as Fig. 1, but the close-up of the $\text{Ly}\alpha$ (upper panel) and $\text{Ly}\beta$ (lower panel) regions. The spectrum is binned by 2 pixels, and 1σ errors are shown by dashed lines with an offset of -0.5 . The wavelength scales of the two panels are chosen so that the $\text{Ly}\alpha$ and $\text{Ly}\beta$ wavelengths at a fixed redshift coincide with each other on the horizontal scale (i.e., $\lambda_{\text{top}}/\lambda_{\text{low}} = \lambda_{\alpha}/\lambda_{\beta}$). The vertical solid line marks the $\text{Ly}\alpha$ and $\text{Ly}\beta$ resonances at $z = 6.295$. The CCD images of the spectrum in the corresponding wavelength ranges are shown at the top and bottom of the figure. The solid and dotted curves are the same with those in Fig. 1. The three dashed curves show the model absorption by the IGM ($z_{\text{IGM,u}} = 6.295$), with $x_{\text{HI}} = 0.01, 0.2, \text{ and } 1.0$, as indicated. The dot-dashed curve is the model absorption by the IGM but with $z_{\text{IGM,u}} = 6.36$ and $x_{\text{HI}} = 1.0$ (the IGM-dominated model).

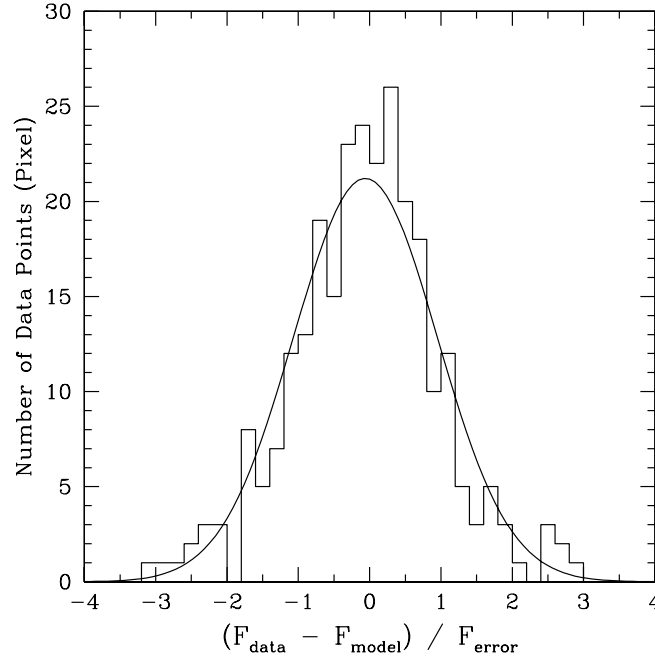


Fig. 3. The histogram for the deviation of the observed flux in a pixel from a model spectrum, normalized by the 1σ error of the data. The reference model is with $\log N_{\text{HI}} = 21.62$, $z_{\text{DLA}} = 6.295$, and $x_{\text{HI}} = 0$ (the DLA-dominated model). There are 268 data points (corresponding to the number of pixels) in the wavelength range used in the fitting analysis. The solid curve is the fit by the Gaussian distribution with $\sigma = 1$.

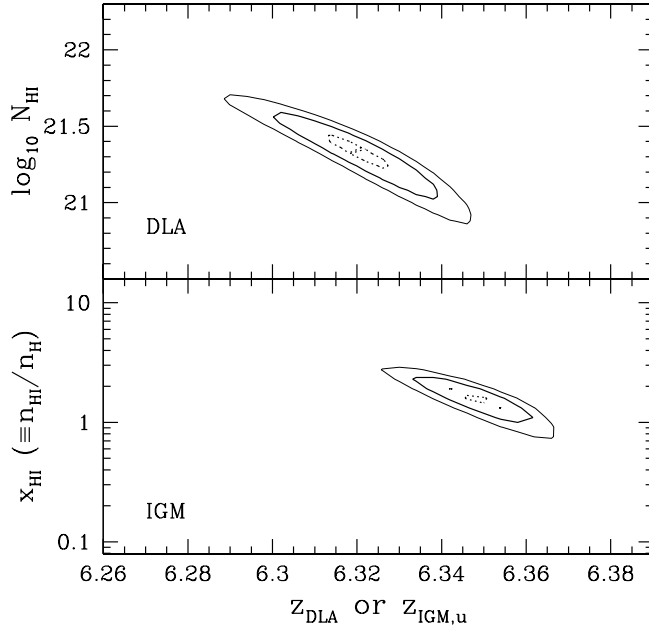


Fig. 4. The arrowed regions for the separate fits of the DLA (upper panel) and IGM (lower panel) absorption models to the red damping wing. The horizontal axis is the DLA redshift (z_{DLA}) for the DLA model but is the upper redshift bound of the extension of neutral hydrogens in the IGM ($z_{\text{IGM,u}}$) for the IGM model. The contours show the levels of $\Delta\chi^2 = 2.30, 9.21$, and 18.4 from the minimum χ^2 , corresponding to 68.3 (dotted), 99 (thick solid), and 99.99% (thin solid) confidence levels for two degrees of freedom. See text (§3) for the reason why the apparently unphysical region of $x_{\text{HI}} > 1$ is also shown. The redshift of metal absorption system and its error are indicated by the thick and thin vertical lines, respectively.

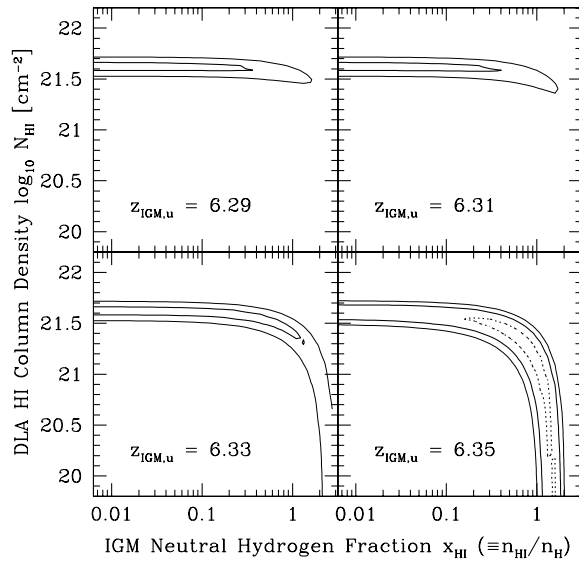


Fig. 5. The arrowed regions for the joint fit of the DLA and IGM absorption models. The four panels are for different values of $z_{\text{IGM,u}}$ as indicated in the panels. The DLA redshift is fixed to $z_{\text{DLA}} = z_{\text{metal}} = 6.295$. The contours show the levels of $\Delta\chi^2 = 3.53, 11.3$, and 21.1 from the minimum χ^2 , corresponding to 95 (dotted), 99 (thick solid), and 99.99% (thin solid) confidence levels for three degrees of freedom. See text (§3) for the reason why the apparently unphysical region of $x_{\text{HI}} > 1$ is shown.

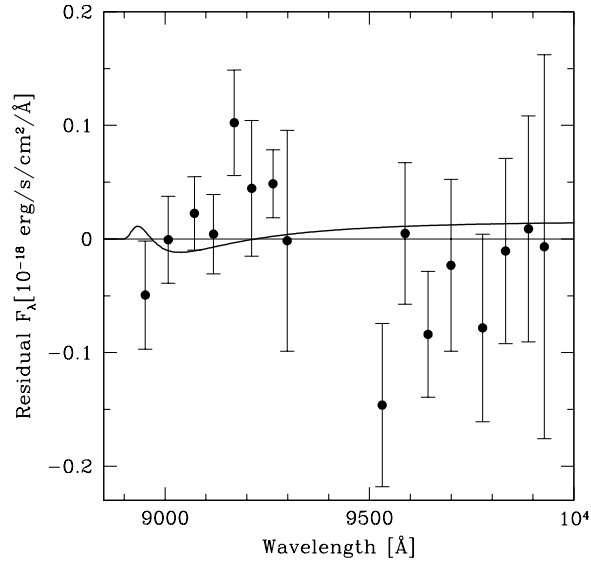


Fig. 6. The model and observed spectra of GRB 050904, in the form of the residual from the DLA-dominated model $[(z_{\text{DLA}}, \log N_{\text{HI}}, z_{\text{IGM,u}}, x_{\text{HI}}) = (6.295, 21.62, 6.295, 0)]$. The connected pixels are binned by up to 20 pixels, after removing the wavelength ranges which were not used in the χ^2 analyses because of absorption features. The thick solid curve is the best-fit model ($\log N_{\text{HI}} = 21.54$) under the constraints of $x_{\text{HI}} = 1$ and $z_{\text{DLA}} = z_{\text{IGM,u}} = 6.295$.

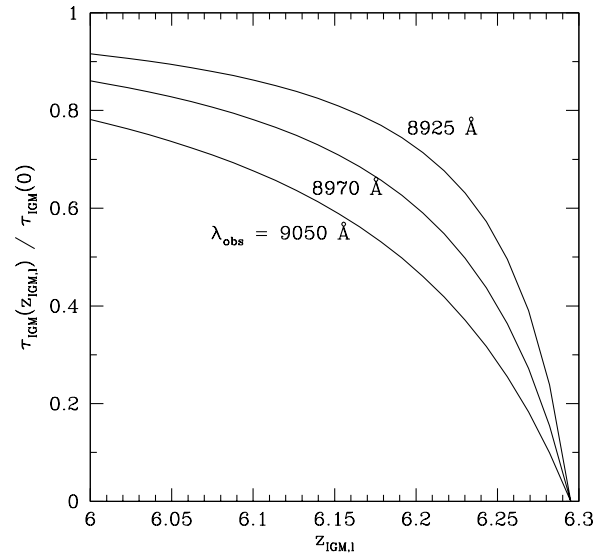


Fig. 7. The IGM optical depth as a function of $z_{\text{IGM},1}$, which is normalized by that at $z_{\text{IGM},1} = 0$, is shown for three values of λ_{obs} as indicated. Here we set $z_{\text{IGM,u}} = 6.295$.

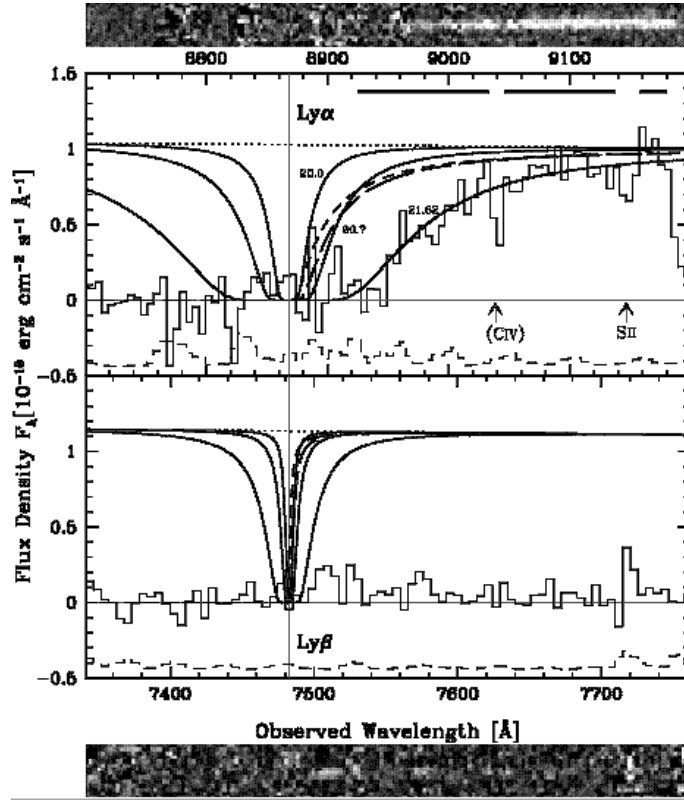


Fig. 8. The same as Fig. 2, but showing some different models. The three solid curves are the model absorption by the DLA at $z_{\text{DLA}} = 6.295$, but with different values of $\log N_{\text{HI}} = 20.0, 20.7$, and 21.62 , as indicated. The short-dashed curve shows the model absorption by the IGM with $z_{\text{IGM,u}} = 6.295$ and $x_{\text{HI}} = 1.0$, and the long-dashed curve is the same but the DLA absorption with $\log N_{\text{HI}} = 20$ and $z_{\text{DLA}} = 6.295$ is added.